Hybrid materials and silica: drastic control of surfaces and porosity of xerogels *via* ageing temperature, and influence of drying step on polycondensation at silicon

Geneviève Cerveau, Robert J. P. Corriu,* Eric Framery, Shubhajit Ghosh and Hubert P. Mutin

Laboratoire de Chimie Moléculaire et Organisation du solide, UMR 5637, Université Montpellier II, cc 007, Place E. Bataillon, F-34095 Montpellier Cedex 5, France. E-mail: cmos@crit.univ-montp2.fr

The effect of drying and ageing conditions on both the degree of polycondensation at silicon and the texture connected with the surface properties (BET, porosity) has been investigated in the case of silica and nanostructured hybrid organic–inorganic solids, obtained by hydrolytic sol–gel performed from a molecular precursor. Various molecular geometries and structural features were investigated using acid or nucleophilic catalysts in MeOH or THF. The aim of this work is first to study the effect of the temperature on the surface properties occurring during the ageing alone which was studied independently of gel formation. The second aim was to consider whether the polycondensation at silicon is influenced by the drying step. The main trend that emerges from these results is the drastic influence of ageing temperature on the texture and porosity of the xerogels. Whereas the level of condensation at silicon is not modified, we observed that higher ageing temperatures favor an increase of the specific surface area and an evolution towards a mesoporosity with narrow pore size distribution, whatever is the level of polycondensation at silicon. In contrast, the drying procedure (transformation of gel into xerogel) induces a significant increase of the level of condensation at silicon (10–14%) when the leaving group of the precursor is OEt, whereas in the case of the OMe group no evolution is observed. The same experimental facts have also been observed in the case of SiO_2.

Introduction

Hydrolytic polycondensation (sol–gel process)[1–3] is a general route for the preparation of organic–inorganic hybrid materials.[4–12] In the course of our studies concerning nanostructured hybrid organic–inorganic materials, we have shown that the parameters that govern the kinetics of polycondensation at silicon control the texture (specific surface area and porosity) of the materials (Scheme 1).[13] Moreover, we have recently pointed out the great importance of the temperature during the ageing step of the solid gel.[14,15] Thus it appears that the final texture of the solid in fact depends on two sets of parameters: one set taking place in solution, which corresponds to the hydrolysis and polycondensation reactions occurring at silicon; the other set being the result of the rearrangements which are occurring in the solid phase during ageing. These results can be connected with observations made in birefringence studies performed on the same materials,[16,17] which show that a micrometric scale anisotropy can be observed only during the ageing of the solid.

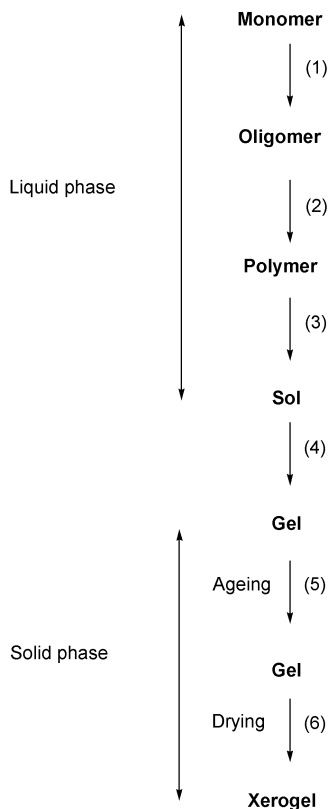These two observations incited us to investigate in more detail the effect of ageing conditions upon the texture of the materials, since both the texture mainly connected with the surface properties of the solid and the structure related to the relative organization of the organic units in the solid are strongly controlled by the reorganization of the material occurring in the bulk of the material.
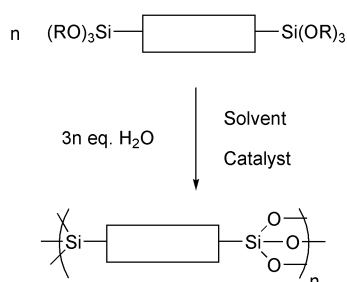
Let us consider now the overall process which transforms the precursor into the xerogel (Scheme 2). We can separate three different transformations. The first one, occurring in solution (steps 1, 2, and 3), is kinetically controlled and is strongly dependent upon the experimental conditions, as previously reported.[13] The second one (step 5) corresponds to ageing which occurs in solid state after the sol–gel transition. Finally, the drying process (step 6) leads to the xerogel. Until now, it has been usual to perform all of the transformations corresponding to steps 1 to 5 at the same temperature (usually room temperature). However, the temperature[14] appeared to be a very drastic factor. Furthermore, it is the only modifiable parameter at this step of the process. We have considered the influence of this parameter independently for the steps occurring in the solid state and in the liquid phase. It was also very important to evaluate the importance of the drying on the properties of the final material. Indeed, recent work has shown the drastic influence of the drying stage on the level of condensation at silicon in the case of SiO_2 formation from TEOS.[18]

The aim of this paper is to make a distinction between the influence of the temperature during solid formation in solution (Scheme 2, steps 1, 2, and 3) and the one able to occur at the surface of the material during the ageing in the solid state (Scheme 2, step 5). Furthermore, we will study the drying effect on the level of condensation at silicon in the case of solids obtained from TMOS and bis-trialkoxysilyl precursors

Scheme 1 Sol–gel process.

Scheme 2 Mechanism of sol–gel process.

evidenced by ^{29}Si NMR studies.[19] Separately, birefringence experiments have confirmed the same result since NaOH is the only catalyst which does not lead to any long range organization evidenced by birefringence.[17]

Experimental

Syntheses of precursors and preparation of the gels were carried out under argon using a vacuum line and Schlenk techniques. THF and MeOH were dried and distilled before use. Compounds 1, 2,[20] 4,[21] 6,[22] 7,[23] 8[20] and 9[24] were prepared according to literature procedures while 3, 5 and 10 were obtained commercially and purified before use. The TBAF (tetrabutylammonium fluoride) solution (1 mol l^{-1} in THF as measured by electrochemistry[25]) and the HCl solution (1 mol l^{-1} in H$_2$O) were commercially obtained and were titrated before use.

Solid-state ^{29}Si CP MAS NMR measurements were performed at room temperature on a Bruker Avance 300 spectrometer operating at 59.6 MHz using a recycling delay of 10 s and a contact time of 5 ms. The spinning rate was 5 kHz in all cases. Chemical shifts are given relative to tetramethylsilane. The experiments were carried out using a 4 mm MAS Bruker probe, zirconia rotors and Kel-F drive caps.

The nitrogen adsorption–desorption isotherms at 77.35 K of the xerogels were recorded on a Micromeritics Gemini III 2375 apparatus. The specific surface area was determined using the BET equation. The pore size distribution was calculated using the BJH method, and the microporous volume was estimated by the t-plot method using the Harkins and Jura standard isotherm.

(Scheme 3). We have selected linear rigid rod precursors 1 and 2, semi-flexible organic units 3 and 4, fully flexible saturated aliphatic precursors 5 and 6, a ferrocene 7 and precursors 8 (rigid) and 9 (flexible) which are presenting respectively three and four directions of polycondensation. We have used acid (HCl) and nucleophilic (TBAF, NMI) conditions in THF and in some cases in MeOH. We did not consider the case of basic catalysis (NaOH), since in this case, we have precedently reported the ability of NaOH to cleave the Si–O–Si bonds

Preparation of silsesquioxane gels for the study of ageing temperature

The preparation of gels was carried out according to the following general procedure. The preparation of xerogel 1Tb is given as an example. To a solution of 2.86 g (9 mmol) of 1 in 9 ml of THF, cooled to −20 °C, was added at −20 °C a solution of 90 µl (90 µmol) of TBAF and 486 µl (27 mmol) of H$_2$O in 8.40 ml of THF. The mixture was kept at −20 °C and after 90 min a monolithic gel formed. Immediately, the gel was
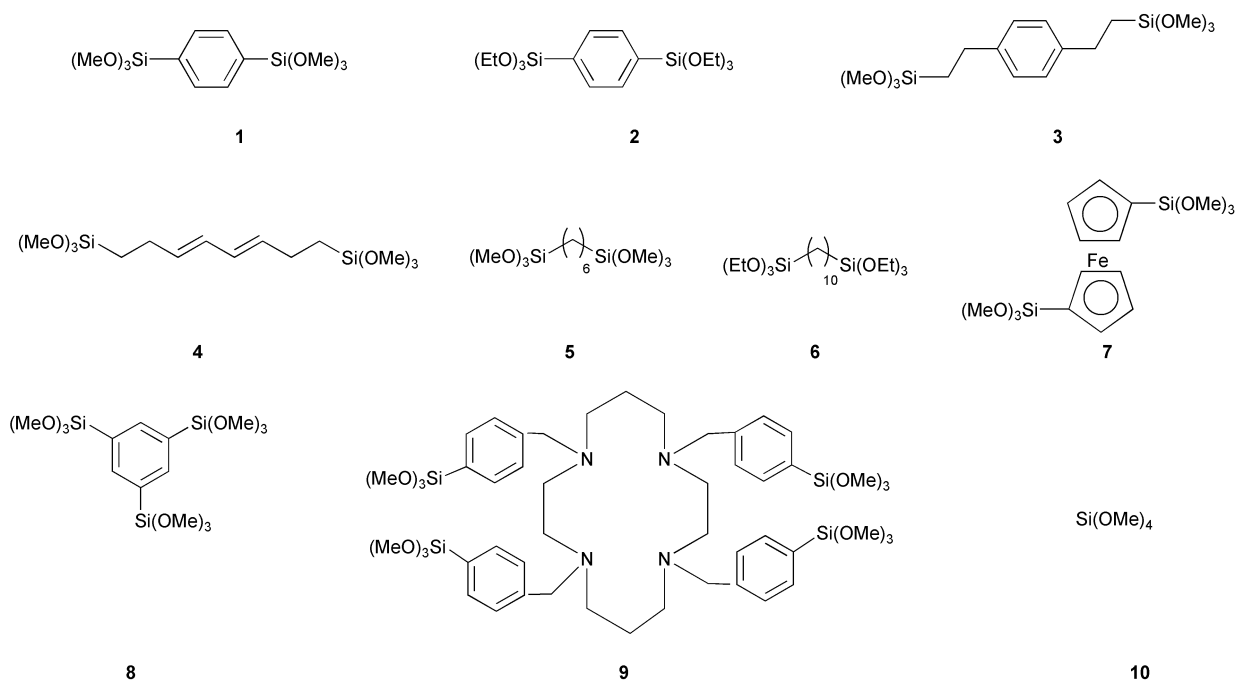
Scheme 3 Molecular precursors.

Table 1 Textural characteristics of xerogels obtained with 1 molar percent of TBAF

Entry	Xerogel	Precursor	Solvent	Temp./°C		BET		
				Gel[a]	Ageing	S.S.A./m² g⁻¹ [b]	μ-Pores (%)[c]	Size/Å[d]
1	**1Ta**	(MeO)₃Si—C₆H₄—Si(OMe)₃	THF	−20	−20	900	55	20–70[e]
2	**1Tb**		THF	−20	+55	1385	5	50
3	**1Tc**		THF	+55	−20	1015	20	20–50[e]
4	**1Td**		THF	+55	+55	1300	5	65
5	**3Ta**	(MeO)₃Si—CH₂—C₆H₄—CH₂—Si(OMe)₃	THF	−20	−20	<10	—	—
6	**3Tb**		THF	−20	+55	715	5	40
7	**3Tc**		THF	+55	−20	700	25	20–60[e]
8	**3Td**		THF	+55	+55	700	5	40
9	**4Ta**	(MeO)₃Si—(chain)—Si(OMe)₃	THF	−20	−20	250	20	20–50[e]
10	**4Tb**		THF	−20	+55	840	5	20–50[e]
11	**4Tc**		THF	+55	−20	620	25	20–60[e]
12	**4Td**		THF	+55	+55	870	5	35, 60
13	**5Ta**	(MeO)₃Si—(CH₂)₆—Si(OMe)₃	THF	−20	−20	<10	—	—
14	**5Tb**		THF	−20	+55	865	0	80
15	**5Tc**		THF	+55	−20	125	40	20–120[e]
16	**5Td**		THF	+55	+55	570	0	20–80[e]
17	**7Ta**	ferrocenyl—Si(OMe)₃ (Fe, (MeO)₃Si—)	THF	−20	−20	<10	—	—
18	**7Tb**		THF	−20	+55	525	45	20–50[e]
19	**7Tc**		THF	+55	−20	220	35	20–80[e]
20	**7Td**		THF	+55	+55	275	40	20–120[e]
21	**8Ta**	(MeO)₃Si—C₆H₃(—Si(OMe)₃)—Si(OMe)₃ (1,3,5)	THF	−20	−20	200	60	20–50[e]
22	**8Tb**		THF	−20	+55	1100	0	20–50[e]
23	**8Tc**		THF	+55	−20	690	25	20–70[e]
24	**8Td**		THF	+55	+55	800	0	20–120[e]
25	**8Ma**		MeOH	−20	−20	575	35	20–50[e]
26	**8Mb**		MeOH	−20	+55	1040	0	70
27	**8Mc**		MeOH	+55	−20	700	20	20–40[e]
28	**8Md**		MeOH	+55	+55	1020	0	80
29	**9Ta**	Cyclam	THF	−20	−20	75	40	20–120[e]
30	**9Tb**	Cyclam	THF	−20	+55	685	35	20–70[e]
31	**9Tc**	Cyclam	THF	+55	−20	300	45	20–40[e]
32	**9Td**	Cyclam	THF	+55	+55	750	15	20–70[e]
33	**10Ma**	Si(OMe)₄	MeOH	−20	−20	800	5	30–50
34	**10Mb**	Si(OMe)₄	MeOH	−20	+55	760	0	80–100
35	**10Mc**	Si(OMe)₄	MeOH	+55	−20	795	0	20–50[e]
36	**10Md**	Si(OMe)₄	MeOH	+55	+55	780	0	90

[a]Temperature of gelation. [b]Specific surface area. [c]Percentage of micropores. [d]Size of mesopores. [e]No narrow pore size distribution.

heated at +55 °C, and aged at this temperature for 6 days. The solid was collected, then ground and washed twice with ethanol, acetone and diethyl ether. The resulting solid was dried at 120 °C *in vacuo* for 3 h yielding 1.95 g of a white powder **1Tb**. The experimental conditions and the textural characteristics of the xerogels obtained from **1**, **3–5** and **7–10** are reported in Table 1.

Preparation of silsesquioxane gels for the study of drying

The preparation of the gels was carried out according to the following general procedure. Preparation of the gel and xerogel obtained from **1** with TBAF is given as an example. To a solution of 1.43 g (4.5 mmol) of **1** in 2.25 ml of THF was added at +20 °C a solution of 45 μl (45 μmol) of TBAF and 243 μl (13.5 mmol) of H_2O in 1.96 ml of THF. A portion of the solution was transferred to a 4 mm ZrO_2 rotor (BL4 Bruker) which was closed with a KEL-F drive cap, and the remaining solution was kept at +20 °C and after few minutes a monolithic gel formed. Then, the gel was aged at the same temperature for 6 days. The gel sample in the rotors was analyzed by ²⁹Si MAS NMR. The remaining gel was collected, then ground and washed twice with ethanol, acetone and diethyl ether. The resulting solid was dried at 120 °C *in vacuo* for 3 h yielding 0.75 g of a white powder. The experimental conditions and the structural characteristics of the xerogels obtained from **1–3**, **5**, **6** and **8** are reported in Table 2.
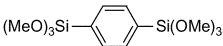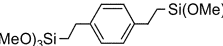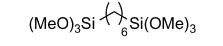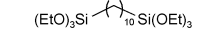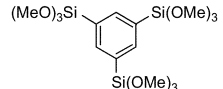
Results and discussion

Influence of ageing temperature

The xerogels were prepared by hydrolytic polycondensation of molecular precursors **1**, **3–5** and **7–9** (Schemes 1 and 3). The concentration of the precursor was 0.5 mol l⁻¹, except for **9** (0.25 mol l⁻¹) and the amount of catalyst was 1 molar percent in all cases. All of the experiments were carried out in THF or MeOH (in the case of **8**) using tetrabutylammonium fluoride (TBAF) as catalyst. The case of tetramethoxysilane (TMOS) **10** was also investigated and the experiments were performed in MeOH. Since a drastic effect of the ageing temperature was observed on the texture of a few xerogels,[26] it was of great interest to extend this observation and to consider the influence of the ageing temperature for various precursors. In this view, two sets of experiments were performed: (i) the gels were prepared at −20 °C, and as soon as they were formed they were aged for 6 days at −20 °C and +55 °C; (ii) the gels were prepared at +55 °C and aged in the same manner at –20 °C and +55 °C. After the usual work-up, the ²⁹Si CP MAS NMR data and textural properties of the xerogels were obtained after drying for 3 h at 120 °C in a vacuum and were compared.

Spectroscopic characterization. The ²⁹Si CP MAS NMR data[22,27,28] of the various xerogels studied did not significantly depend upon the ageing temperature. The T^1 [C–Si(OR)₂(OSi)], T^2 [C–Si(OR)(OSi)₂] and T^3 [C–Si(OSi)₃] substructures were

Table 2 Comparison of structural characteristics of gels and xerogels

| | | | | | | 29Si NMR (%) | | | | | | | | | | |
| | | | | | | Gel | | | | | Xerogel | | | | | |
Entry	Precursor	Solvent	Catalyst	Temp./°C[a]	Ageing/days	T^0	T^1	T^2	T^3	L.C.[b]	T^0	T^1	T^2	T^3	L.C.[b]
1	(MeO)₃Si—⟨benzene⟩—Si(OMe)₃	THF	TBAF	+20	6	0	17	46	37	73	0	18	35	47	76
2		THF	HCl	+20	6	0	36	64	0	55	0	43	42	15	57
3		THF	NaOH	+20	6	10	23	38	29	62	10	27	29	34	62
4		THF	NMI	+20	6	9	31	32	28	60	14	29	33	24	56
5		MeOH	TBAF	−20	6	0	25	48	27	67	0	28	49	23	65
6		MeOH	TBAF	+20	6	0	26	51	23	66	0	26	49	25	66
7		MeOH	TBAF	+55	6	0	20	57	23	68	0	23	48	29	69
8	(EtO)₃Si—⟨benzene⟩—Si(OEt)₃	THF	TBAF	+20	6	0	14	44	42	76	0	0	31	69	89
9		THF	HCl	+20	6	0	34	52	14	60	0	14	60	26	70
10	(MeO)₃Si—⟨benzene⟩—Si(OMe)₃	THF	TBAF	+20	6	0	0	34	66	89	0	0	35	65	88
11	(MeO)₃Si—(CH₂)₆—Si(OMe)₃	THF	HCl	+20	0	0	42	52	6	55	0	40	54	6	55
12		THF	HCl	+20	2	0	17	64	19	67	0	20	55	25	68
13		THF	HCl	+20	4	0	18	64	18	67	0	18	64	18	67
14		THF	HCl	+20	6	0	15	71	14	66	0	15	71	14	66
15		THF	HCl	+20	30	0	9	67	24	72	0	8	67	25	72
16	(EtO)₃Si—(CH₂)₁₀—Si(OEt)₃	THF	HCl	+20	0	0	38	62	0	54	0	24	48	28	68
17		THF	HCl	+20	2	0	45	55	0	52	0	32	53	15	61
18		THF	HCl	+20	4	0	35	55	10	58	0	26	51	23	66
19		THF	HCl	+20	6	0	30	58	12	61	0	23	51	26	68
20		THF	HCl	+20	30	0	6	69	25	73	0	3	63	34	77
21	(MeO)₃Si—⟨benzene 1,3,5⟩—Si(OMe)₃, Si(OMe)₃	THF	TBAF	+20	6	2	34	48	16	60	0	34	46	20	62
22		THF	HCl	+20	6	0	40	54	6	55	0	34	59	7	57

[a] Temperature of gelation and ageing. [b] Level of condensation.

observed in all cases (Fig. 1). The percentage of the different substructures T^n was estimated by deconvolution of the spectra and these values were used to estimate the level of condensation at silicon.[29] CP MAS spectroscopy is not quantitative. However, it has been shown that single pulse experiments did not reveal any significant variation in the relative peak intensity from the CP MAS spectra in the cases of this kind of compound.[22,28,30] The results obtained in all cases showed that the degree of condensation at silicon was poorly influenced by the temperature of ageing. The 29Si CP MAS NMR spectra of xerogels shown in Fig. 1 illustrate these results.

Textural properties of the xerogels. The specific surface areas[31] of the xerogels were determined using 35 point adsorption–desorption isotherm plot measurements and were evaluated using the BET equation.[32] The porous volume was
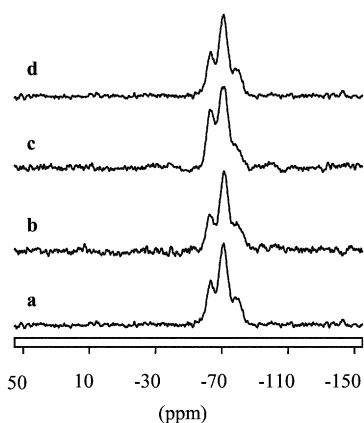

Fig. 1 29Si CP MAS NMR spectra: (a) **8Ma**, (b) **8Mb**, (c) **8Mc**, (d) **8Md**.

determined by the BJH method[33,34] and the microporous volume was evaluated by the analysis of the t-plot diagram.[35,36] The results reported in Table 1 clearly show how much the textural properties and mainly the porosity of the xerogels were dependent upon the temperature of ageing. For example, a comparison between the four xerogels **1Ta**, **1Tb**, **1Tc** and **1Td** (Table 1, entries 1–4) pointed out the drastic influence of the temperature of ageing on the texture of the xerogels. The specific surface areas were very high for all of these xerogels; however, increasing the ageing temperature induced an increase of the BET surface. The xerogels **1Ta** and **1Tc** presented very similar porosities: the shape of the adsorption–desorption isotherms was the same, indicating a largely microporous solid with a low mesoporous contribution. The microporous volume represented 55% (**1Ta**) and 20% (**1Tc**) of the total porous volume and the mesopores exhibited no narrow pore size distribution. In the same way, the xerogels **1Tb** and **1Td** also had similar textural characteristics: the N₂ adsorption–desorption isotherms were the same, and the solids were mesoporous with a narrow pore size distributions of 50 Å (**1Tb**) and 65 Å (**1Td**). This result could be indicative of a control of the texture of the xerogels during the ageing, the ageing temperature being an important parameter. The influence of the ageing temperature has been studied in the case of the molecular precursors **1**, **3**–**5** and **7**–**9** (Scheme 3). The same drastic influence as described in the case of **1** was observed for the other precursors (Table 1): a low ageing temperature (−20 °C) favored the formation of solids mainly microporous with a weak mesoporous contribution without narrow pore size distribution; in contrast, a higher ageing temperature (+55 °C) led to mesoporous solids with high specific surface areas and narrow pore size distributions. The N₂ adsorption–desorption isotherms of xerogels **8Ma**–**d** shown in Fig. 2 illustrate this result. The experiments performed in the
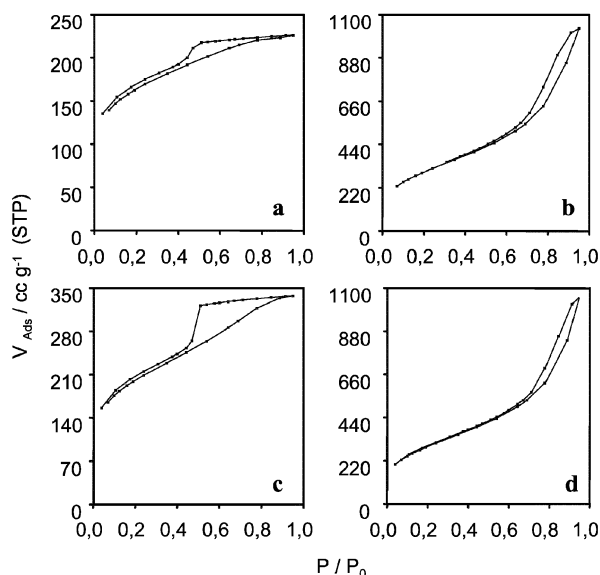
Fig. 2 N$_2$ adsorption–desorption isotherms: (a) **8Ma**, (b) **8Mb**, (c) **8Mc**, (d) **8Md**.

case of TMOS **10** led to similar results. The silica xerogels exhibited high specific surface areas in all cases (Table 1, entries 33–36). Only 5% of micropores were present and mesopores exhibited no narrow pore size distribution when the whole process was performed at −20 °C. The silica-gels were mesoporous in the other cases, and when the whole process was performed at +55 °C, mesopores of 90 Å were observed. Fig. 3 shows the N$_2$ adsorption–desorption isotherms obtained for **10Ma–d**.

The main trend, which emerges from these results, is the drastic influence of ageing temperature on the texture and porosity of the xerogels. An increase of the specific surface area and an increase of the mesoporosity were generally observed when the gels were aged at a higher temperature. In most of the cases, a narrow pore size distribution was also observed. This effect was also evidenced in the case of silica-gels. In contrast, the temperature of ageing as shown previously on the temperature of gelation and length of ageing does not influence the polycondensation at silicon.
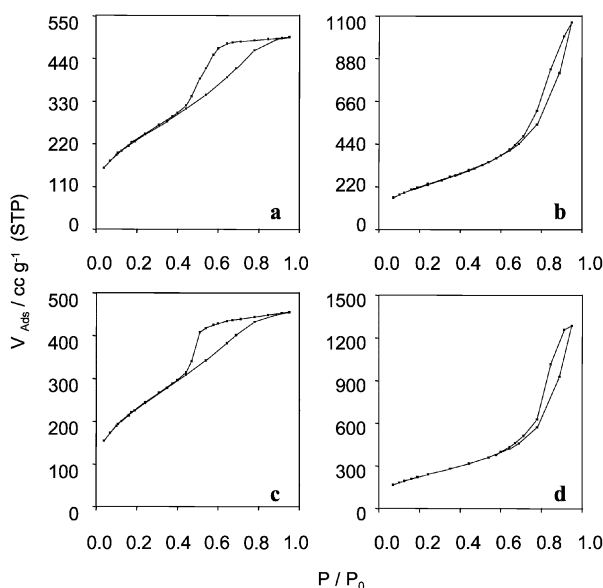

Fig. 3 N$_2$ adsorption–desorption isotherms: (a) **10Ma**, (b) **10Mb**, (c) **10Mc**, (d) **10Md**.

Influence of drying step (gel → xerogel)

The influence of drying was studied in the case of organic precursors **1**, **2**, **3**, **5**, **6** and **8** (Scheme 3). The precursors **2** and **6** bearing triethoxysilyl groups were investigated in order to determine the possible influence of the leaving group at silicon. The concentration of the precursor was 1 mol l^{-1} in THF. In the case of **1**, **2**, **3** and **8**, the gels were prepared at +20 °C and aged for 6 days at this temperature. Several catalysts were used: ionic and non-ionic nucleophiles, acid, base in THF. Some experiments were also performed in MeOH using TBAF at different temperatures (Table 2). In the case of precursors **5** and **6**, the catalyst was HCl and the gels were aged for various periods. The gelation conditions and the ^{29}Si CP MAS NMR data of the gels and the corresponding xerogels are given in Table 2.

For a given precursor, when the leaving group was OMe, the gels and the xerogels exhibited very similar ^{29}Si CP MAS NMR data under the same experimental conditions (catalyst, temperature, length of ageing). The different T^n site populations as well as the overall level of condensation at silicon were roughly identical for the gel and the corresponding xerogel (Table 2, entries 1–7, 10–15 and 21–22). These results show that no change occurred during the washing and drying steps. In contrast, when the leaving group was OEt (as in the case of **2** and **6**), an influence of these steps has been evidenced. When **2** was hydrolyzed in THF with TBAF, the gel exhibited T^1, T^2 and T^3 substructures corresponding to a 76% level of condensation at silicon, whereas the xerogel presented only T^2 and T^3 substructures and an 89% level of condensation at silicon (Table 2, entry 8). The ^{29}Si CP MAS NMR spectra of gels and xerogels obtained from **1** and **2** in THF with TBAF shown in Fig. 4 illustrate this result. When the catalyst was HCl, the same effect was observed (Table 2, entry 9). In the same way, in the case of **6** the gels were aged for various periods of time; interestingly, in all cases the degree of condensation of the xerogels was significantly higher than that of the gels (the difference was roughly 10%). For each gel, the T^1 site population decreased whereas those for T^3 increased (Table 2, entries 16–20). In this case, we are comparing the evolution of a solid where the vicinity of the protons is always the same with respect to the silicon atom, since we are studying modifications which do not affect the geometry of the organic group. The transformation of the gel into the xerogel concerns only the surface, and the NMR spectrometry analyses all the silicon atoms of the solid.

A similar observation has been reported in the case of HCl-catalyzed hydrolysis of tetraethoxysilane (TEOS): a noticeably
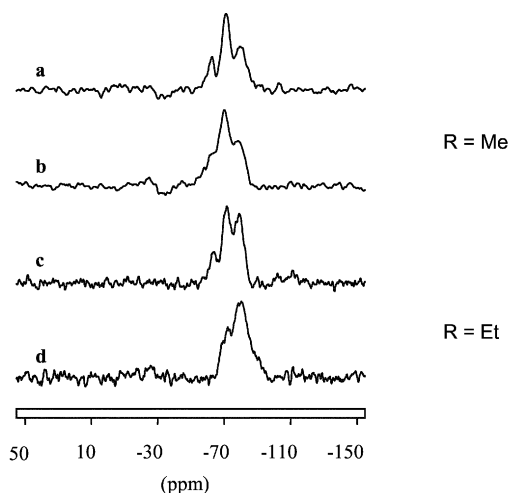

Fig. 4 ^{29}Si CP MAS NMR of gel (a, c) and xerogel (b, d) obtained from **1** or **2** in THF with TBAF.

higher degree of condensation at silicon of the xerogel compared to that of the gel was evidenced.[18]

Conclusion

The results presented here point out the following facts.

(1) The drying step can be of drastic importance following the nature of the leaving group at silicon. An important evolution of polycondensation at silicon was observed when OEt is used as leaving group. However, in the case of OMe, the polycondensation at silicon did not exhibit any evolution during the drying procedure. Thus all the results and conclusions that we have reported in the preceding papers remain unchanged since we have always worked with Si(OMe)$_3$ groups for the formation of the polysilsesquioxane network. However, this observation is of importance for all the solids obtained from OEt or O^{i}Pr used as leaving groups, since the global polycondensation at silicon is modified during the drying step.

(2) Our experiments have evidenced the drastic importance of ageing temperature. During this step, the solid undergoes a reorganization of the surface, which modifies drastically the pore size distribution and influences the specific surface area. In all cases, an increase of the temperature induces the disappearance of the microporosity and favors the trend to a monodisperse mesoporosity. We can propose that these changes are the result of the redistribution reactions involving the surface of the solid.

(3) These redistributions are occurring without a significant modification of polycondensation at silicon, since no change is observed in NMR experiments.

References and notes

1 J. Livage, *Chem. Scr.*, 1988, **28**, 9.
2 J. Rouxel, *Chem. Scr.*, 1988, **28**, 33.
3 C. J. Brinker and G. W. Scherer, *Sol–Gel Science: The Physics and Chemistry of Sol–Gel Processing*, Academic Press, London, 1990.
4 L. L. Hench and J. K. West, *Chem. Rev.*, 1990, **90**, 33.
5 *New J. Chem.*, special issue, 1994.
6 D. A. Loy and K. J. Shea, *Chem. Rev.*, 1995, **95**, 1431.
7 U. Schubert, N. Hüsing and A. Lorenz, *Chem. Mater.*, 1995, **7**, 2010.
8 P. Judenstein and C. Sanchez, *J. Mater. Chem.*, 1996, **6**, 511.
9 R. J. P. Corriu, *Angew. Chem., Int. Ed.*, 2000, **39**, 1376.
10 D. A. Loy, J. P. Carpenter, T. M. Alam, R. Shaltout, P. K. Dorhout, J. Greaves, J. H. Small and K. J. Shea, *J. Am. Chem. Soc.*, 1999, **121**, 5413.
11 K. J. Shea and D. A. Loy, *Chem. Mater.*, 2001, **13**, 3306.
12 K. J. Shea and D. A. Loy, *Acc. Chem. Res.*, 2001, **34**, 707.
13 G. Cerveau, R. J. P. Corriu and E. Framery, *Chem. Mater.*, 2001, **13**, 3373.
14 G. Cerveau, R. J. P. Corriu and E. Framery, *J. Mater. Chem.*, 2000, **10**, 1617.
15 G. Cerveau, R. J. P. Corriu and E. Framery, *Chem. Commun.*, 1999, 2081.
16 B. Boury, R. J. P. Corriu, V. Le Strat, P. Delord and M. Nobili, *Angew. Chem., Int. Ed.*, 1999, **38**, 3172.
17 F. Ben, B. Boury, R. J. P. Corriu and V. Le Strat, *Chem. Mater.*, 2000, **12**, 3249.
18 E. Framery and P. H. Mutin, *J. Sol Gel Sci. Technol.*, 2002, **24**, 191.
19 G. Cerveau, R. J. P. Corriu and E. Framery, *C.R. Acad. Sci. Paris, Ser. IIc*, 2001, **4**, 79.
20 R. J. P. Corriu, J. Moreau, P. Thépot and M. Wong Chi Man, *Chem. Mater.*, 1992, **4**, 1217.
21 G. Cerveau, R. J. P. Corriu and B. Dabiens, *J. Mater. Chem.*, 2000, **10**, 1113.
22 H. W. Oviatt Jr., K. J. Shea and J. H. Small, *Chem. Mater.*, 1993, **5**, 943.
23 G. Cerveau, C. Chuit, E. Colomer, R. J. P. Corriu and C. Reyé, *Organometallics*, 1990, **9**, 2415.
24 G. Dubois, PhD Thesis, Université Montpellier II, Montpellier - France, 1999.
25 D. A. Skoog, D. M. West and F. J. Holler, *Fundamentals of Analytical Chemistry*, Saunders College Publishing, New York, 1992.
26 G. Cerveau, R. J. P. Corriu and E. Framery, *J. Mater. Chem.*, 2001, **11**, 713.
27 H. Marsmann, in *^{29}Si NMR Spectroscopic Results*, P. Diehl, E. Fluck and M. Kosfeld, ed., Springer Verlag, Berlin, 1981, p. 65.
28 G. Cerveau, R. J. P. Corriu, C. Lepeytre and P. H. Mutin, *J. Mater. Chem.*, 1998, **8**, 2707.
29 The level of condensation has been evaluated according to the following formula: level of condensation = [0.5(area T^1) + 1.0(area T^2) + 1.5(area T^3)]/1.5.
30 K. J. Shea, D. A. Loy and O. Webster, *J. Am. Chem. Soc.*, 1992, **114**, 6700.
31 S. J. Gregg and S. W. Sing, *Adsorption, Surface Area and Porosity*, Academic Press, London, 1982.
32 S. Brunauer, P. H. Emmett and E. J. Teller, *J. Am. Chem. Soc.*, 1938, **60**, 309.
33 S. Brunauer, L. S. Deming, W. S. Deming and E. J. Teller, *J. Am. Chem. Soc.*, 1940, **62**, 1723.
34 E. P. Barrett, L. S. Joyner and P. P. Halenda, *J. Am. Chem. Soc.*, 1951, **73**, 373.
35 W. D. Harkins and G. Jura, *J. Chem. Phys.*, 1943, **11**, 431.
36 B. C. Lippens and J. H. deBoer, *J. Catal.*, 1965, **4**, 319.